An Intelligent Direct power control for Power Ripple Mitigation of DFIG based WECS

Megha Vyas[1], Vinod Kumar Yadav[2]
[12]Department of (Electrical Engineering)
[12](College of Technology and Engineering / MPUAT / Research Scholler)
(Udaipur, Rajasthan, India 313001)

Abstract

For a doubly-fed induction generator (DFIG) based wind energy conversion system, this research offers an adaptive neuro fuzzy inference system (ANFIS) maximum power point tracking (MPPT) controller (WECS). This research proposes an enhanced control method for wind generation systems' rotor and grid side converters. Direct power control (DPC) has grown in popularity as a result of its simple control structures and quick dynamic responsiveness. However, because of other controllers in active and reactive power, it has a drawback of large ripple in active and reactive power and delayed reaction. The simulation findings were confirmed using the MATLAB/Simulink environment on a 2 MW wind turbine. The controller's performance is compared to that of a traditional controller under various input/output conditions.

Keywords: DFIG, WECS, DPC, ANFIS, GSC, RSC, MPPT

1. Introduction

Due to rising electrical energy demand and environmental concerns, significant effort is being undertaken to generate power from renewable energy sources. The availability and lack of hazardous emissions are two main advantages of adopting renewable energy sources. Wind turbines are undoubtedly the most developed renewable energy source, with commercial wind turbine ratings now topping 9 MW. It is also the most cost-effective of all the world's environmentally pure and safe renewable energy sources. It is environmentally benign in the sense that every 1 kWh of power generated by wind reduces CO2 emissions by 1 kilogram, and the operation of a 50-tones wind turbine eliminates the burning of 500 tones-of coal per year.

Because of the aforementioned benefits, the total installed capacity of wind power in the global market is rapidly increasing. Even if 10% of the world's raw wind potential could be used, all of the world's electrical demands would be supplied, according to estimates. Of course, the fundamental disadvantage of wind power is that its availability is rather random, and it must be supplemented by other sources to meet demand [1].

India's energy policy is defined by the country's growing energy deficit and increased emphasis on developing alternative energy sources, particularly nuclear, solar, and wind. Around 70% of India's energy generation capacity is based on fossil fuels, with coal accounting for 40% of total energy consumption, followed by crude oil and natural gas at 24% and 6%, respectively. India is heavily reliant on fossil fuel imports to cover its energy needs. By 2030, India's energy import dependence is predicted to exceed 53% of total energy consumption. [2]

India is one of the world's fastest expanding energy markets, and it is predicted to be the secondlargest contributor to global energy demand growth by 2035, accounting for 18% of the total increase in worldwide energy consumption. India is the world's fifth largest wind power market, with ambitions to add roughly 20GW of solar capacity by 2022. Within 25 years, India wants to raise nuclear power's contribution to overall energy generation capacity from 4.2 percent to 9 percent. The country is building five nuclear reactors (the third most in the world) and aims to build 18 more nuclear reactors (the second most in the world) by 2025. A wind energy conversion system (WECS), which consists of a wind turbine (WT), an electric generator, a power electronic converter, and the accompanying control system, can harness wind energy. Different WECS structures can be created depending on the components used. The goal of all constructions, however, is the same: wind energy must be transformed to electric power at grid frequency at variable wind velocities. [3]

Variable-speed wind turbine operation is advantageous for wind energy conversion systems because it produces 10% to 15% more output energy while lowering wind turbine costs. Since the late 1990s, the doubly-fed induction generator (DFIG) based variable speed wind energy conversion system (WECS) has been the leading technology in the market. This position has changed in recent years due to the evolution of WECS trends toward larger power capacity, increased power density, reduced cost per kW, and the requirement for higher reliability. Furthermore, DFIG necessitates the use of a gearbox to match the turbine and rotor speeds, which is prone to failure and requires routine maintenance, making the system unreliable [4].

The maximum amount of energy that can be extracted from wind is determined by both the wind's strength and the energy conversion system's operational point. As a result, in WECS, the Maximum Power Point Tracking (MPPT) is critical not only to improve the system's efficiency but also to reduce the installation cost's return period. The aim of MPPT in a WECS is to optimize the generator speed in relation to the wind velocity intercepted by the wind turbine in order to maximize power. The information about generator rotor position/speed and wind speed must be acquired using well-calibrated mechanical sensors such as encoders/resolvers and anemometers. Mechanical sensors, on the other hand, raise the cost, failure rate, and hardware complexity of WECS. [5] P&O control, optimal torque (OT) control, power signal feedback (PSF) control, wind speed estimation (WSE)-based control, and fuzzy logic (FL) control are the five basic categories of wind speed sensor-less MPPT control systems now available. [6-8]

Because it does not require any prior knowledge of the system and is completely independent of wind speed statistics and wind turbine characteristics, the P&O approach, also known as the hill-climb search (HCS) method, is frequently used in WECS to search for the maximum power point. By perturbing the control variable and noting the consequent rise or reduction in power, a simple hill climbing control is applied in this manner. If the perturbation results in a rise in power, the same perturbation is applied to the next control instance; if not, the sign of the perturbation is flipped to track in the direction of rising power.

Proportional a generic control loop feedback controller can also be used with an integral controller. This is the most common feedback controller, and it's employed in a variety of industrial control applications. The discrepancy between a measured process variable and a target point is used by the PI controller to calculate an "error" value. The controller adjusts the method control inputs to try to mitigate the error. The controller conducts the control action by analyzing power, reactive power, coefficient of power, and speed fluctuations. The membership function in the FLC controller defines the input variables to the fuzzy rule base and the output variables to the controlled plant. The purpose of a fuzzy rule base is to hold information about how a domain's process works. [9]

The pitch angle of a wind turbine is controlled by an adaptive neuro fuzzy interference system (ANFIS) controller at different wind speeds. It's a phony neural system based on the TakagiSugeno fuzzy induction framework with an IF-THEN arrangement for inexact non-linear capabilities. As a result, ANFIS is regarded to be a comprehensive estimator. It captures the benefits of both neural systems and fuzzy rational standards in a single framework because it coordinates both. The ANFIS controller compares the reference parameters to the DFIG voltage, phase angle, and frequency. The error between the two is then submitted to ANFIS, which reduces the value of the error to nearly zero. [10]

The DPC strategy with the use of an intelligent controller has been studied in this study. The use of the adaptive neural fuzzy inference system (ANFIS) MPPT scheme with a three-phase induction generator, as well as simulation evaluation of this unique control system, are the original contributions. The key benefits of the DPC-ANFIS control scheme are its ease of implementation and lower active and reactive power ripples when compared to other control schemes. To reduce the ripple content in reactive and active powers, the DPC-ANFIS-MPPT approach is applied.

2. Modelling of DFIG WECS

Because of their tremendous efficiency, DFIGs are now the most used power generation technology. The rotor of the DFIG is connected to the back-to-back converter, while the stator is connected to the power grid. The rotor side control (RSC) and grid side control (GSC) are each given their own control loop [11]. Literatures [11-14] have described various DPC control strategies for DFIG. DPC has several advantages, including quick reaction of active and reactive powers and ease of implementation. Pulse width modulation (PWM) and space vector pulse width modulation (SVPWM) switching techniques are utilized to control the frequency and output voltage of the drives [16, 17].

The SVPWM approach has the capacity to minimize harmonic content while maintaining acceptable switching losses. Feedforward compensation is employed in this control technique to provide decoupling between the q-axis and d-axis currents, making the DFIG model easier to solve and allowing the use of PI controllers [14]. This control approach, on the other hand, results in higher total harmonic distortion (THD), active/reactive power ripple, and torque ripple in DFIG-based wind turbines. A schematic diagram for DFIG-based WECS is shown in Figure 1.

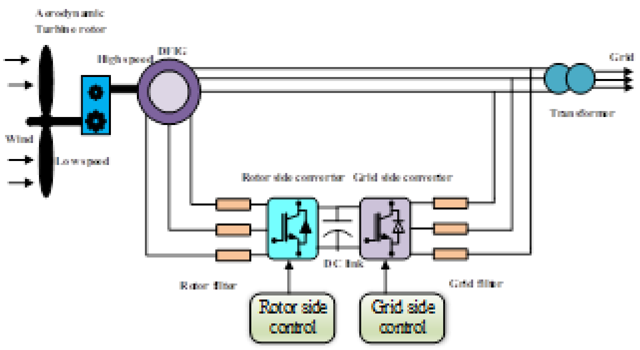

Fig.1 DFIG-based WECS

The direct power control technique entails direct control of active and reactive powers, which must fall into two distinct bands in order to be applicable. Controlling two parameters, the stator active and reactive powers, is the straightforward goal. Those quantities are directly controlled in control strategy by selecting the appropriate vector state converter. Several research publications on the DPC scheme of the permanent magnet synchronous generator (PMSG) [24, 25] and the DFIG [16-18] have been published.

[29] has presented a DPC system based on an expected stator flow. The accuracy of the stator flux estimation can be guaranteed because the stator voltage is largely harmonics free.

The fundamental disadvantage of conventional control technique is the unfixed switching frequency. The super-twisting sliding mode (STSM) algorithm is used in the DPC strategy [30]. A DFIG-based wind energy system (WES) with a DPC control method based on artificial neural networks (ANNs) [31]. The actual and active power of DFIG-based WECS are controlled using a discrete sliding mode control [32]. The DFIG is controlled using a combination of second order sliding mode control (SOSMC) and fuzzy logic controller (FLC) [33]. [34] provided a DPC technique for a DFIG-based wind power generating system employing a seven-level SVPWM strategy. The goal of DFIG's vector control is to establish an equivalent system to that of DC machines [35], i.e., decoupled active and reactive power regulation. Because of its simplicity, indirect vector control is the most widely employed. [36]

Decoupling is done at the output of the rotor current regulators with feedback from the system in this way. Because it provides for the adjustment of the powers, it is distinguished from a control by loop in cascade of the power and rotor current for each axis, because it allows for closed loop control of the currents Ird, Irq and the powers Qs, Ps. The associated reference voltages Vrd and Vrq are generated using the indirect vector control method. The rotor reference voltages are calculated using a Park transformation. Figure 2 shows a vector control approach.

The equations of fluxes and voltages for the DFIG stator and rotor in Park orientation structure are given by [21-23]:

$$V_{ds} = R_s I_{ds} + \frac{d}{dt}\Psi_{ds} - \omega_s \Psi_{qs} \quad (1)$$

$$V_{qs} = R_s I_{qs} + \frac{d}{dt}\Psi_{qs} + \omega_s \Psi_{ds} \quad (2) \; V_{dr} = R_r I_{dr} + \frac{d}{dt}\Psi_{dr} - \omega_r \Psi_{qr} \quad (3)$$

$$V_{qr} = R_r I_{qr} + \frac{d}{dt}\Psi_{qr} + \omega_r \Psi_{dr} \quad (4)$$

Where: Vdr, and Vqr are the rotor voltages.

Vqs and Vds are the stator voltages.

Ids and Iqs are the stator currents.

Idr, and Iqr are the rotor currents.

The stator and rotor flux can be expressed as:

$$\Psi ds = LsIds + MId \quad (5)$$

$$\Psi_{qs} = L_s I_{qs} + MI_{qr} \quad (6)$$

$$\Psi dr = LrIdr + MIds \quad (7)$$

$$\Psi qr = LrIqr + MIqs \quad (8)$$

Where: M: is the mutual inductance. ψdr and ψqr are the rotor fluxes. ψds and ψqs are the stator fluxes.

The reactive and active powers can be written as:

$$P_s = \frac{3}{2}(V_{ds} I_{ds} + V_{qs} I_{qs}) \quad (9)$$

$$Q_s = \frac{3}{2}(V_{qs} I_{ds} - V_{ds} I_{qs}) \quad (10)$$

Where: Ps: is the active power. Qs: is the reactive power.

Where: Ω: is the mechanical rotor speed. J: is the inertia. Tr: is the load torque.

f: is the viscous friction coefficient.

$$T_{em} = \frac{3}{2} p \frac{M}{L_s}(\Psi_{qs} I_{dr} - \Psi_{ds} I_{qr}) \quad (11)$$

p: number of pole pairs

T_{em}: electromagnetic torque

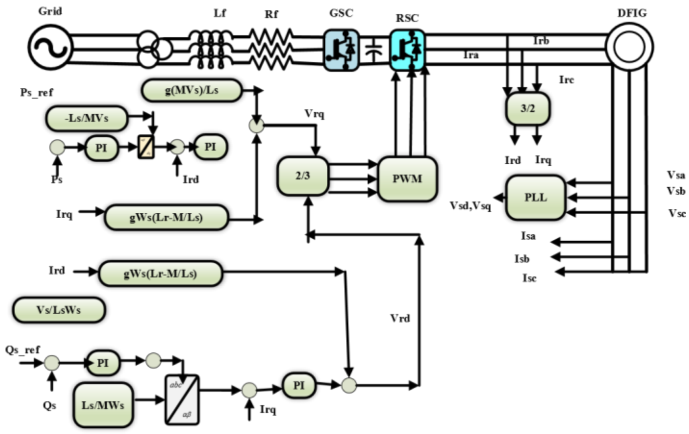

Fig. 2 Vector control

3. DPC with ANFIS Controller

Direct Power Control (DPC) is an electrical machine control system based on the concept of direct torque control. In an SVPWM rectifier, the purpose is to control active and reactive power directly. Two comparators that detect the switching state of semiconductors with the help of a switchboard and the value of the sector where the generator voltage is measured introduce inaccuracies between the reference values of the instantaneous active and reactive powers and their measurements [24-25]. Figure 3 shows the DPC control scheme of a DFIGbased wind turbine with the use of the ANFIS-MPPT controller. The stator reactive and active powers are controlled by the rotor side converter in this control scheme.

A neural network is used in ANFIS to tune a fuzzy logic Sugeno type controller. The intelligent controller's performance is satisfactory, with enhanced estimate efficiency. The ANFIS-MPPT controller is designed using MATLAB/Simulink software. The ANFIS controller is trained using the intelligent controller editor toolkit. The steps for designing the converter control circuit are as follows. [37-41]

Step 1: Data from the traditional SVPWM approach is put into the ANFIS controller.

Step 2: The output of the ANFIS is assessed.

Step 3: The ANFIS controller's FIS data is imported.

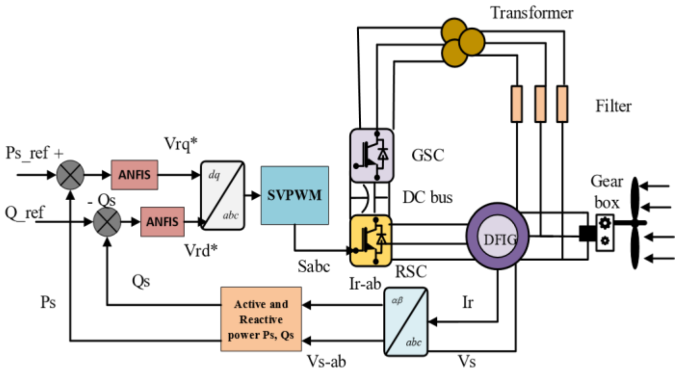

Fig.3 DPC of ANFIS controller

Step 4: FIS data is exported to the proposed converter control circuit's fuzzy logic controller.

Figure 3 depicts the schematic structure of an ANFIS controller. The circle denotes fixed nodes, while the square denotes adaptive nodes.

ANFIS comprises two input nodes, x1 and x2, which represent DC link voltage and change in DC link voltage of the converter control circuit, respectively, as shown in Fig.4. There are five input layers and one output layer in the controller structure.

Layer 1: The inputs x1 and x2 are triangle membership functions (MF). ANFIS controllers are frequently equipped with bell-shaped MF.

Layer 2: By accepting the input from the first layer and combining it with the corresponding weight, the weight of the membership function (MF) is determined. The resulting fuzzy sets (MF) are utilized to represent the input parameters x1 & x2.

Layer 3: The third layer is also known as the Rule layer. The number of layers and the number of fuzzy rules is assumed to be equal when fuzzy rule matching is conducted. Then each rule's activation level and normalized weight for each node are assessed.

Layer 4: The defuzzification procedure is followed. The output is generated by deducing fuzzy rules. Fuzzy singletons produce a collection of Neuro-Fuzzy parameters, which are denoted by weighted connections between the Rule and Defuzzification layers.

Layer 5: All incoming signals are added together, and the result is evaluated.

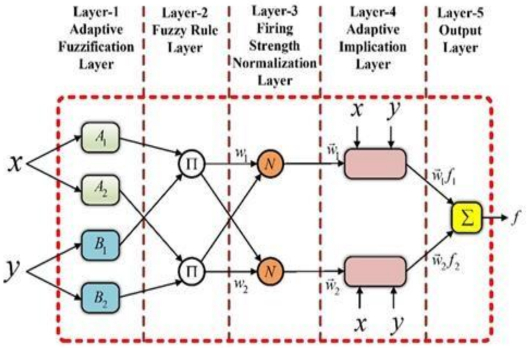

Fig.4 Schematic diagram of ANFIS controller

Table 1 shows the ANFIS rules for the proposed system. Figures 5 and 6 show the membership function definition. For membership purposes, we utilize the following terms:

NB: Negative Big, NM: Negative Middle, NS: Negative Small, PS: Positive Small, PB:

Positive Big, EZ: Equal Zero, PM: Positive Middle. NB: Negative Big, NM: Negative Middle, NS: Negative Small, PS: Positive Small, PB: Positive Big, EZ: Equal Zero, PM: Positive Middle.

Table 1 ANFIS Rules

e/Δe	NB	NM	NS	EZ	PS	PM	PB
NB	NB	NB	NB	NB	NM	NS	EZ
NM	NB	NB	NB	NM	NS	EZ	PS
NS	NB	NB	NM	NS	EZ	PS	PM
EZ	NB	NM	NS	EZ	PS	PM	PB
PS	NM	NS	EZ	PS	PM	PB	PB
PM	NS	EZ	PS	PM	PB	PB	PB
PB	EZ	PS	PM	PB	PB	PB	PB

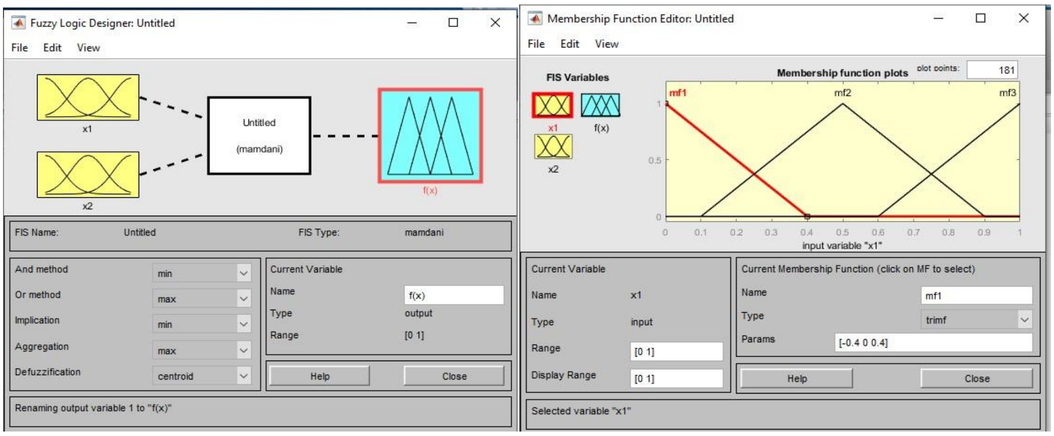

(a) **(b)**

Fig.5 Input variable membership function

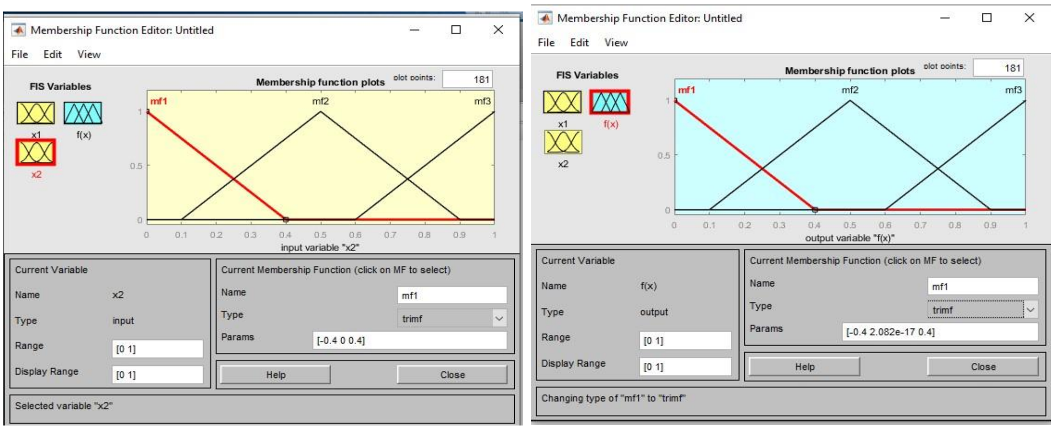

(a) (b)

Fig. 6 Output variable membership function

4. Result and analysis

4.1 Response during Steady-State Condition

For the proposed converter interfaced DFIG for WECS, Figure.7(a) presents simulation results for grid linked mode based on the adaptive neuro fuzzy control maximum power point tracking control. The waveforms for 50 Hz grid voltage and current, grid active and reactive power, fictional dc link voltage, and generator speed are displayed in the results. Grid phase voltage and current are sinusoidal and perfectly balanced with unity power factor, according to the simulated results of Figure.7. The filter capacitor is responsible for the small phase leg. The total harmonic distortion (THD) of the grid voltage and current has been proven to be less than 5%, which is within the IEEE-519 standards' permitted limits.

WECS, a created back-to-back converter interface, was tested using MATLAB/Simulink and SimPower System Toolbox under various phases of ground faults, which generate system dips. At time t= 0.04s, three phases to ground, three phase short circuit, and single phase to ground fault are applied near the grid for a length of 0.02s. The behavior of fictional dc link voltage and grid currents throughout the fault period must be investigated in order to determine the developed WECS' ride-through capabilities. Figures 7(b) depict the planned converter interfaced grid connected WECS's simulated reaction during fault circumstances.

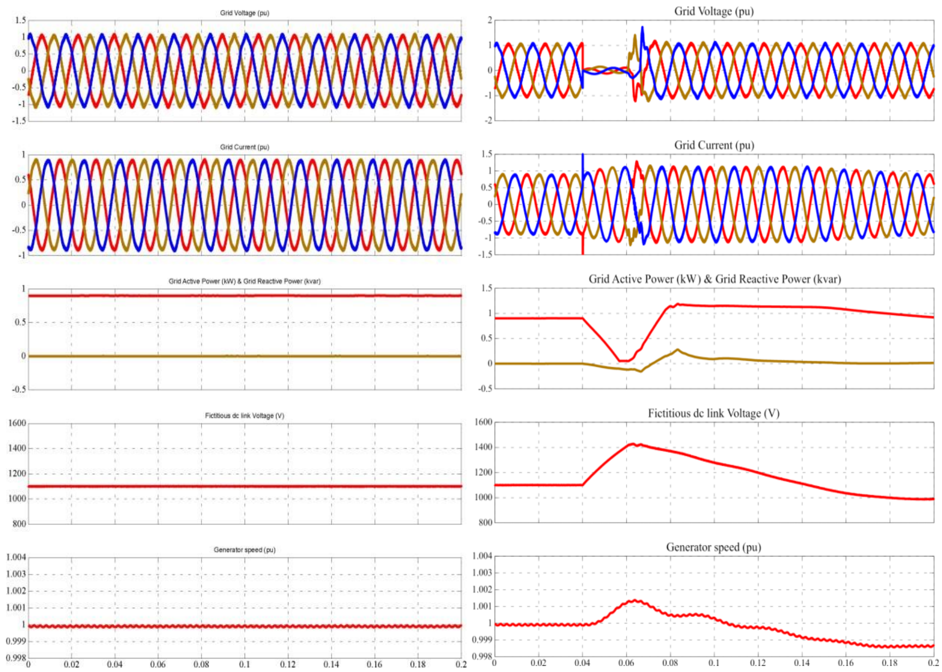

(a) (b) Fig.7: Simulated responses during steady-state & three phases to ground fault condition. Grid voltage (pu), grid current (pu), grid active power (kW), grid reactive power (kvar), fictitious dc link voltage (V), generator speed (pu)

4.2 Response under Varying Wind Speed Condition

The response to varying wind speeds is modelled. The system is replicated with a sudden reduction in wind speed followed by a fast increase. Response of a system with a wind velocity that fluctuates with a mean value near 9 m/s and reduces to a mean value near 7.5 m/s at 0.28 s after an almost step shift. The wind speed abruptly increases to 12 m/s after a few milliseconds. Figures 8(a) and (b) demonstrate the phase voltage, current, and power of a wind generator as the wind speed decreases and increases.

The control effect, which adjusts the firing delay angle of the converter in response to changes in system frequency, is primarily responsible for the constant local frequency and voltage. As changes in system frequency are substantially controlled, the values of output real power from the generator reduce or increase appropriately as the wind velocity lowers or increases. The control system gives an order for corresponding decrease or increase of power.

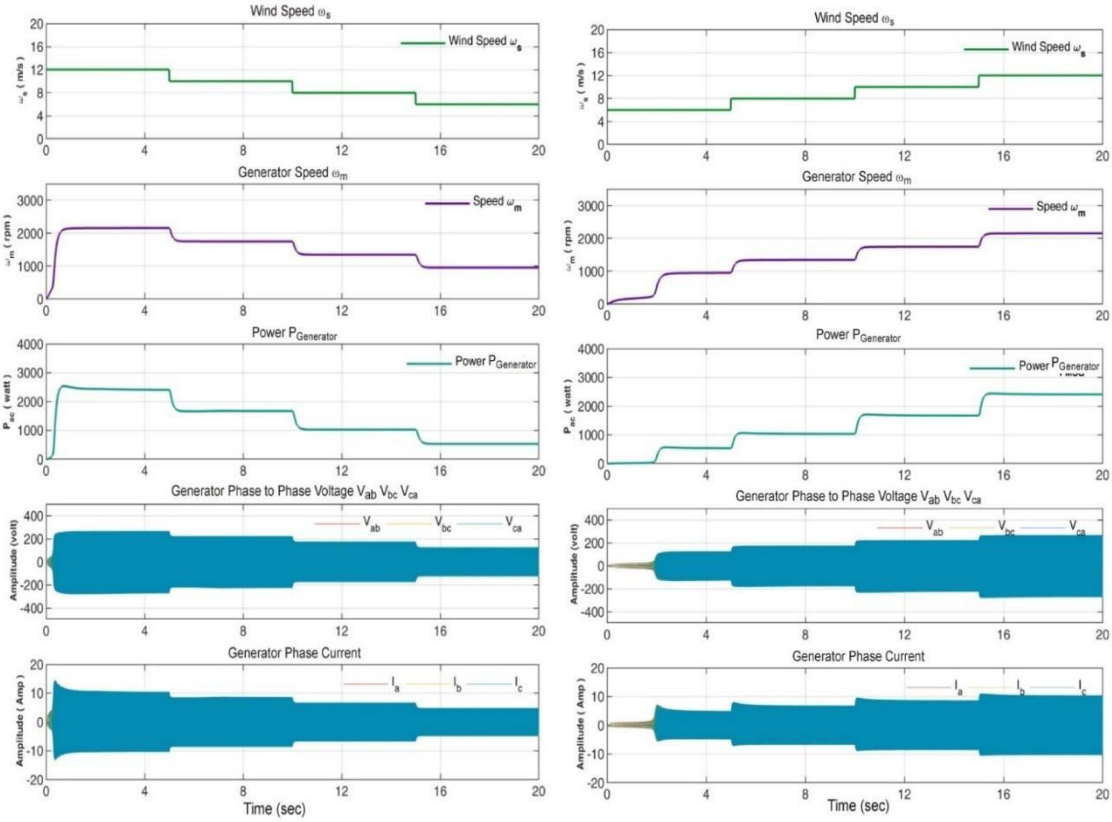

(a) **(b)**

Fig. 8: Wind Generator Phase Voltage, Current & Power at Decreasing & Increasing Wind Speed

Back-to-back converter interfaced DFIG based WECS are simulated under three-phase and single-phase faults to confirm the superiority of dynamic performance of the proposed adaptive neural fuzzy control system over conventional controls. The simulated waveforms of converter voltage, grid current, grid frequency, grid voltage, grid active power, and fictional dc link voltage are shown in Figures.9.

Figure 9 shows the simulation results of the proposed control method versus conventional control under three-phase failure. Figure 9(a) shows how, with the proposed adaptive neural fuzzy control, the grid voltage recovers completely in 0.5 seconds after the fault, meeting grid codes and preventing the wind turbine from tripping. Furthermore, the modelled waveforms in Figure.9(a) reveal that the WECS is not electrically stressed, as a result of which it remains connected during and after the fault, boosting the system's transient stability. WECS' current also stays well below the limit.

The grid frequency is also marginally influenced, indicating that the malfunction hasn't put the wind turbine under any stress. In addition, as seen by the waveform in Figure. 9, the grid voltage remains unaltered (a). As shown in Figure 9(a), the active power produced by the WECS takes a tiny dip and recovers in less than 0.35s, meeting the grid code requirement. Figure 11(b) depicts the system's response under conventional control for the same three-phase fault event. The traditional control, as can be shown, does nothing to mitigate fault oscillations, and the system recovers slowly.

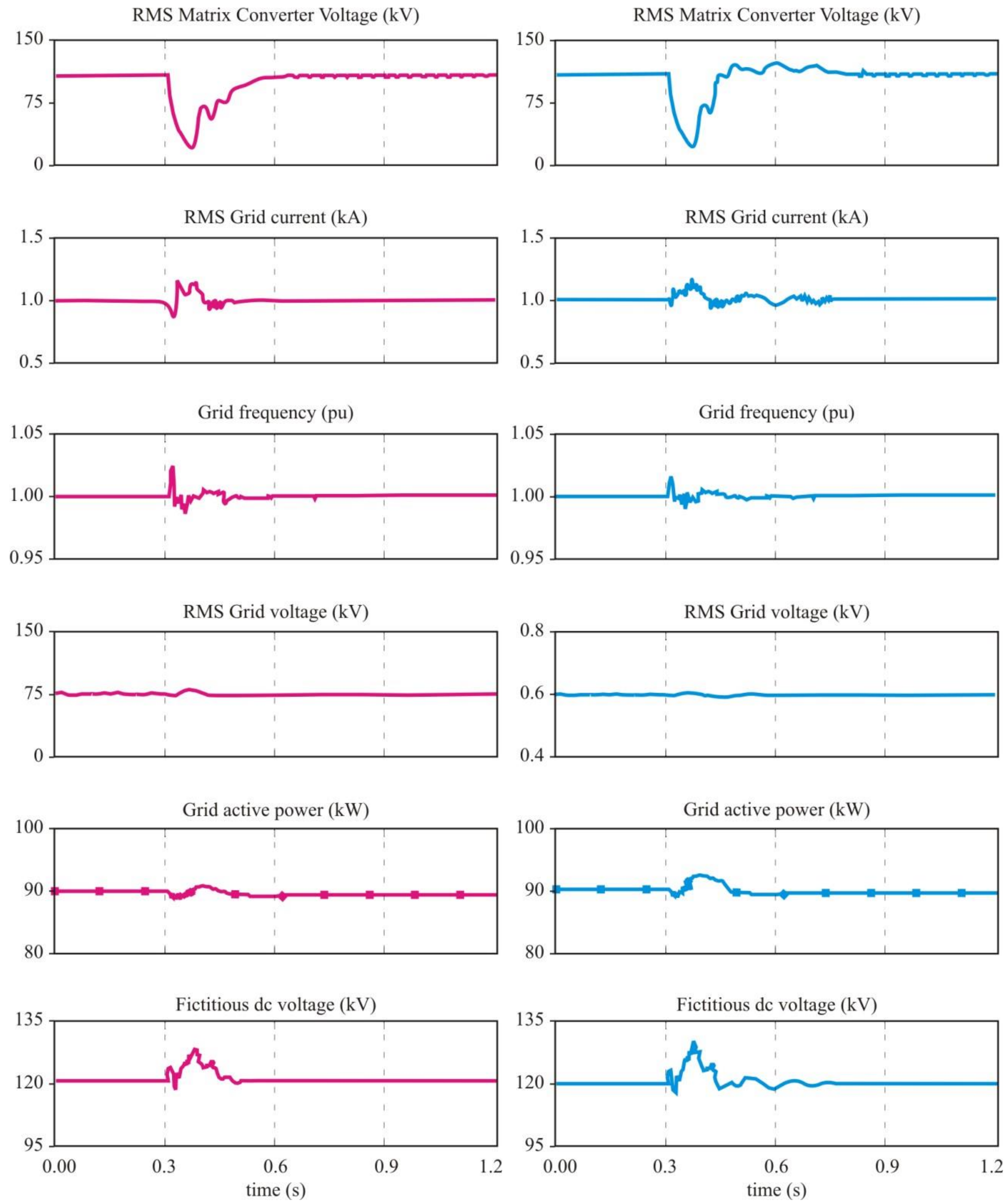

(a) proposed control (b) conventional control Fig. 11: Simulated response of the proposed converter interfaced WECS under threephase fault. (Where waveforms are of RMS converter voltage, RMS grid current, grid frequency, grid voltage, grid active power, and fictitious dc link voltage

Conclusion

For DFIG-based WECS, this paper proposed an adaptive neural fuzzy inference system maximum power point tracking controller. For peak power point tracking, the controller has incorporated an ANFIS. In MATLAB/Simulink, the suggested controller has implemented a 2 MW variable speed wind turbine. With a wide range of wind speed conditions, the ANFIS technique resulted in smoother power and lowered the conventional approach, according to a comparison analysis. In this paper, a DPC-ANFIS-MPPT controller is developed to improve the performance of the control strategy by reducing active and reactive power ripple.

References

1. Polinder, H., Bang, D., Van, R., McDonald, A. S. and Mueller, M.A. 2007. 10 MW Wind Turbine Direct-Drive Generator Design with Pitch or Active Speed Stall Control. IEEE International on Electric Machines & Drives, 2:1390-1395.
2. Freries, L.L. 1990. Wind energy conversion systems. Prentice Hall, New York, USA.
3. Ackermann, L.S.T. 2000. Wind Energy Technology and current status. a review. Renewable and Sustainable Energy Review, 4:315-375.
4. Bansal, R.C., Zobaa, A.F. and Saket, R.K. 2005. Some Issues Related to Power Generation Using Wind Energy Conversion Systems: An Overview. International Journal of Emerging Electric Power Systems, 3(2):1-19.
5. Hansen, A.D., Iov, F., Blaabjerg, F. and Hansen, L.H. 2011. Review of contemporary wind turbine concepts and their market penetration. J. Wind Eng., 58(4):1081-1095.
6. Kazmi, S. M.R., Goto, H., Guo, H. J. and Ichinokura, O. 2011. A Novel Algorithm for Fast and Efficient Speed-Sensorless Maximum Power Point Tracking in Wind Energy Conversion Systems. IEEE Transactions on Industrial Electronics, 58(1):29-36.
7. Abdullah, M.A., Yatim, A.H.M., Tan, C.W. and Saidur, R. 2012. A review of maximum power point tracking algorithms for wind energy systems. Renewable & Sustainable Energy Review, 16(5):3220-3227.
8. Musunuri S. and Ginn, H.L. 2011. Comprehensive review of wind energy maximum power extraction algorithms. In Proceeding of IEEE Power and Energy Society General Meeting, 1-8.
9. [19] U. Datta, J. Shi, A. Kalam and J. Li, "DFIG Pitch Angle Control with PID-type Fuzzy Logic Controller in a Microgrid," 2020 15th IEEE Conference on Industrial Electronics and Applications (ICIEA), 2020, pp. 258-263.
10. [20] M. M. M. Ali, A. Youssef, G. Abdel-Gaber and A. S. Ali, "Adaptive Fuzzy-PID Based Pitch Angle Control of Wind Turbine," 2018 Twentieth International Middle East Power Systems Conference (MEPCON), 2018, pp. 1110-1114.
11. Wa, Y., Yang, W. Different control strategies on the rotor side converter in DFIG-based wind turbines, Energy Procedia, Elsevier, Vol. 100, pp. 551-555, 2016.
12. Amrane, F. – Chaiba, A. – Babas, B. – Mekhilef, S.: Design and implementation of high-performance field-oriented control for grid-connected doubly fed induction generator via hysteresis rotor current controller, Rev. Roum. Sci. Techn-Electrotechn. Et Energ, Vol. 61, No. 4, pp. 319-324, 2016.
13. Amrane, F. – Chaiba, A.: A novel direct power control for grid-connected doubly fed induction generator based on hybrid artificial intelligent control with space vector modulation, Rev. Roum. Sci. Techn.-Electrotechn. Et Energ, Vol. 61, No. 3, pp. 263-268, 2016.
14. Boudjema, Z. – Taleb, R. – Djerriri, Y. – Yahdou, A.: A novel direct torque control using second order continuous sliding mode of a doubly fed induction generator for a wind energy conversion system, Turkish Journal of Electrical Engineering & Computer Sciences, Vol. 25, pp. 965-975, 2017.
15. Jou, S. – Lee, S. – Park, Y. – Lee, K.: Direct Power Control of a DFIG in Wind Turbines to Improve Dynamic Responses, Journal of Power Electronics, Vol. 9, No. 5, pp. 781 790, 2009.
16. Tavakoli, S. M. – Pourmina, M. A. – Zolghadri, M.R.: Comparison between different DPC methods applied to DFIG wind turbines, International Journal of Renewable Energy Research, Vol. 3, No. 2, pp. 446-452, 2013.
17. Mirzakhani, A. – Ghandehari, R. – Davari, S. A.: A New DPC-based Control Algorithm for Improving the Power Quality of DFIG in Unbalance Grid Voltage Conditions, International Journal of Renewable Energy Research, Vol. 8, No. 4, pp. 2229-2238, 2018.
18. Singh, B. – Naidu, N. K. S.: Direct power control of single VSC-based DFIG without rotor position sensor, IEEE Transactions on Industry Applications, Vol. 50, No. 6, 2014.
19. Shehata, E. G. – Salama, G. M.: Direct power control of DFIGs based wind energy generation systems under distorted grid voltage conditions, Electr. Power Energy Syst. Vol. 53, pp. 956-966, 2013.
20. Leon, A. E., Member, S., Mauricio, J. M., & Member, S. (2020). Mitigation of Sub-synchronous Control Interactions Using Multi-Terminal DC Systems. IEEE Transactions on Sustainable Energy, 3029.
21. Benbouhenni, H. – Boudjema, Z. – Belaidi, A.: Direct vector control of a DFIG supplied by an intelligent SVM inverter for wind turbine system, Iranian Journal of Electrical and Electronic Engineering, Vol. 15, No. 1, pp. 45-55, 2019.
22. BenbouhennI, H. – Boudjema, Z. – Belaidi, A.: Direct vector command based on three-level NSVM of a doubly fed induction generator for wind energy conversion, IEEE Xplore, 2019.
23. Benbouhenni, H. – Boudjema, Z. – Belaidi, A.: DFIG-based wind turbine system using three-level neural space vector modulation technique, Majlesi Journal of Mechatronic Systems, Vol. 7, No. 2, pp. 35-45, 2018.
24. Gao, S., Member, S., Zhao, H., Member, S., Gui, Y., Member, S., Zhou, D., Member, S., & Blaabjerg, F. (2020). An Improved Direct Power Control for Doubly Fed Induction Generator. IEEE Xplore, 8993(c), 1–14.
25. Mirzakhani, A. (2021). Performance improvement of DPC in DFIGs during unbalanced grid voltage based on extended power theory. Science Direct, November 2020, 1–33.

26. Kashkooli, M. R. A., Madani, S. M., Member, S., & Lipo, T. A. (2019). Improved Direct Torque Control for a DFIG under Symmetrical Voltage Dip with Transient Flux Damping. IEEE Transactions on Industrial Electronics Improved, 0046(c), 0278–0046.

27. Kamel, O. M. (2019). Evaluating Dynamic Performance of DTC under Grid Disturbance for a Wind Driven DFIG. 2019 21st International Middle East Power Systems Conference (MEPCON), 213–219.

28. Li, L., & Nian, H. (2018). Direct Power Control of DFIG System Without Phase-Locked Loop Under Unbalanced and Harmonically Distorted Voltage. IEEE Transactions on Energy Conversion, 33(1), 395–405.

29. Mazouz, F., Belkacem, S., Colak, I., Drid, S., & Harbouche, Y. (2020). Electrical Power and Energy Systems Adaptive direct power control for double fed induction generator used in wind turbine. Electrical Power and Energy Systems, 114(May 2019), 105395.

30. Kumar, C. E. S., Jasper, J., & Pregitha, R. E. (2018). Soft Computing Techniques Used Power Quality Enhancement of Doubly Fed Induction Generator Based Wind Energy Conversion System. Taga Journal Swansea Printing Technology Ltd, 14, 2785–2798.

31. Amin, I. K., Uddin, M. N., Hannan, M. A., & Alam, A. H. M. Z. (2019). Adaptive Neuro-fuzzy Controller for Grid Voltage Dip Compensations of Grid Connected DFIG-WECS. IEEE Xplore, 2101–2106.

32. Amin, I. K., Uddin, M. N., & Marsadek, M. (2019). ANFIS Based Neuro-Fuzzy Control of DFIG for Wind Power Generation in Standalone Mode. IEEE International Electric Machines & Drives Conference (IEMDC), 2077–2082.

33. Automatisés, S., Benbouhenni, H., Boudjema, Z., Belaidi, A., Nationale, E., & Maurice, O. (2020). DPC Based on ANFIS Super-Twisting Sliding Mode Algorithm of a Doubly-Fed Induction Generator for Wind Energy System. Journal Européen des Systèmes Automatisés V, 53(1), 69–80.

34. Moghadam, H. M., Gheisarnejad, M., & Esfahani, Z. (2020). A Novel Supervised Control Strategy for Interconnected DFIG-Based Wind Turbine Systems: MiL Validations. IEEE Transactions on Emerging Topics in Computational Intelligence, 1–10.

35. H. Nian, P. Cheng, and Z. Q. Zhu, “Independent operation of DFIGbased WECS using resonant feedback compensators under unbalanced grid voltage conditions,” IEEE Trans. Power Electron., vol. 30, no. 7, pp. 3650–3661, Jul. 2015.

36. Cheng, P., Nian, H., Member, S., Wu, C., & Zhu, Z. Q. (2017). Direct Stator Current Vector Control Strategy of DFIG Without Phase-Locked Loop During Network Unbalance. 32(1), 284–297.

37. Benbouhenni, H. Belaidi, A., Boudjema, Z. (2020). Power ripple reduction of DPC DFIG drive using ANN controller. Acta Electrotechnica et Informatica, 20(1), 15–22.

38. Jyothi, P., Prakash, R. B. R., & Varma, P. S. (2020). Application of artificial intelligence to DFIG based wind farm for reactive power compensation. International Journal of Renewable Energy Research, 10(2), 955–966.

39. Adel, A. H., Abo-zaid, S., & Elwany, M. (2021). Harmonics Reduction using a Modified Controller for Doubly Fed Induction Generator. International Journal of Recent Technology and Engineering (IJRTE), 9(5), 45–50.

40. Eltamaly, A. L. I. M. (2020). Dynamic Control of a DFIG Wind Power Generation System to Mitigate Unbalanced Grid Voltage. IEEE Access, 8, 39091–39103.

41. Moreira, A. B., André, T., Santos, D. O. S., Siqueira, V., Teixeira, D. E. C., Souza, R. R. D. E., Paula, M. V. D. E., Member, S., & Filho, E. R. (2019). Control of Powers for Wind Power Generation and Grid Current Harmonics Filtering from Doubly Fed Induction Generator: Comparison of Two Strategies. IEEE Access, 7, 32703–32713.